

Evaluation of liquefaction potential in reworked volcanic-colluvial deposits of the Bawen Area, Semarang Regency

Desiana Vidayanti^{1*}, Ramli Nazir², Ratnaningsih¹, Det Komerdevi¹, Pintor Tua Simatupang¹, Eka Nur Fitriani¹,

¹Faculty of Engineering, Mercu Buana University, Jakarta, Indonesia

² Faculty of Engineering, University of Technology Malaysia, Johor Bahru, Malaysia

Article Info

Article history:

Received:

September 8, 2025

Revised:

November 2, 2025

Accepted:

November 6, 2025

Available online:

November 30, 2025

Keywords:

Liquefaction;

SPT data;

CSR-CRR;

Factor of Safety;

Semarang Regency;

Abstract

Liquefaction is a major geotechnical hazard that can severely damage infrastructure in earthquake-prone areas. This study evaluates the liquefaction potential of volcanic-colluvial deposits in Semarang Regency, Central Java, using Standard Penetration Test (SPT) data and the Simplified Procedure of Seed and Idriss (1971). Cyclic Stress Ratio (CSR) and Cyclic Resistance Ratio (CRR) were computed to obtain Factors of Safety (FS) under three earthquake scenarios ($M_w = 5.0, 5.9,$ and 6.5). Results show that for $M_w = 6.5$, the shallow sandy layers at 0-3 m have $FS = 0.07-0.21$ (highly susceptible), while the 4.5-9 m interval is $FS = 0.8-0.96$ (marginal to near-threshold) and the >10 m strata remain stable ($FS > 1.2$). For $M_w = 5.9$, shallow liquefaction is confined to 0-3 m ($FS = 0.09-0.27$), with the 4.5-9 m zone showing $FS = 1.0-1.2$ (marginal to stable). Even for $M_w = 5.0$, the 0-3 m layer yields $FS = 0.14-0.41$, indicating liquefaction susceptibility, whereas deeper layers are stable ($FS > 1.0-1.2$). These findings indicate that loose, saturated silty-sand layers with shallow perched groundwater are the most critical to cyclic softening. The site is underlain by reworked volcanic-colluvial materials derived from Mount Ungaran, characterized by fine-grained, near-saturated deposits within the upper 10 m. Compared with previous studies in northern Semarang, this study highlights the moderate liquefaction susceptibility of southern volcanic-colluvial terrains, an area rarely analyzed in Central Java and provides practical insights for toll-road foundation design and mitigation strategies in similar geological settings.

Corresponding Author:

Desiana Vidayanti

desiana@mercubuana.ac.id



Copyright © 2025 Desiana Vidayanti, Ramli Nazir, Ratnaningsih, Det Komerdevi, Pintor Tua Simatupang, Eka Nur Fitriani
Licensee Universitas Islam Indonesia

Introduction

Indonesia is one of the countries with a high level of vulnerability to earthquakes because it is located at the convergence of three major tectonic plates: the Indo-Australian, Eurasian, and Pacific plates. This tectonic condition causes the country to frequently experience earthquakes of various magnitudes, which can trigger serious geotechnical problems, one of which is liquefaction. Liquefaction occurs when saturated soil experiences an increase in

pore water pressure due to cyclic loading, resulting in a loss of shear strength and causing the soil to behave like a liquid. This phenomenon can lead to large ground deformations, settlement, lateral spreading, loss of bearing capacity, and even the collapse of infrastructure built on it. The 2018 Palu liquefaction event, for example, caused massive infrastructure failures, ground displacements of more than 200 meters, and significant casualties (Gallant et al., 2020; Kusumah, 2018; Nurdin, 2019; Widiyanto et

al., 2019). Similar incidents were also reported in Niigata (1964), Kobe (1995), and Christchurch (2011), demonstrating the seriousness of the liquefaction hazard for infrastructure resilience in earthquake-prone areas (Jefferies & Been, 2016).

The study area lies on the southern margin of the Semarang Basin, composed of fine-grained volcanic and colluvial materials derived from the Ungaran volcanic complex. These deposits are classified as reworked volcanic-colluvial materials (Qcv), indicating that the original volcanic products have undergone secondary transport and redeposition by surface runoff and slope processes. This reworking produces loose, fine-grained sandy-silty layers that often exhibit high moisture content and variable density. Previous investigations in the northern and coastal parts of Semarang (Agustina, 2024; Widiarso et al., 2025) reported very soft to medium alluvial soils with shallow groundwater levels (< 2 m) that exhibit a high liquefaction potential. In contrast, the Bawen area represents the transitional volcanic-colluvial terrain at the foot of Mount Ungaran, where deposits are dominated by reworked silty sand, clayey sand, and tuffaceous layers. Geological and hydrogeological studies in the Ungaran sector (Kusumayudha et al., 2011) indicate complex subsurface stratification and variable groundwater depths (2-5 m), which correspond well with the stratigraphy and partial saturation conditions observed at the present site.

Evaluating liquefaction potential is essential before designing foundations or transportation infrastructure in earthquake-prone areas. Soil that undergoes liquefaction can lose its bearing capacity, causing differential settlement, lateral deformation, and disruption of infrastructure services, which in turn lead to significant socio-economic losses (Wicaksono et al., 2024). Studies on the Solo-Yogyakarta-NYIA Kulonprogo and Serang-Panimbang Toll Roads revealed several segments with Factors of Safety (FS) < 1 , making them

highly susceptible to liquefaction during major earthquakes. Therefore, liquefaction potential evaluation at the design stage is critical for determining appropriate mitigation strategies. Various countermeasures, such as soil densification, stone columns, or deep foundations, have been applied successfully in both local and international projects (Huang et al., 2016a, 2016b; Moderie & Rippe, 2009; Pal & Deb, 2018; Salem et al., 2017). These measures not only improve structural safety but also reduce post-earthquake repair costs.

Liquefaction potential evaluation is not only relevant for toll roads but also has a wider impact on the design of other transportation infrastructure such as railways and ports. A comprehensive risk-based approach is needed to map the likelihood of ground failure and its impact on transportation networks. Recent studies (Can et al., 2024; D'Apuzzo et al., 2020; Fajarwati et al., 2025) have shown that liquefaction can also disrupt railway and port operations, confirming the need for comprehensive risk-based evaluation across transportation networks.

Field soil conditions are generally layered, consisting of combinations of sand, silt, and clay with a shallow groundwater table. This stratigraphic characteristic significantly influences liquefaction potential because inter-layer interactions can determine the distribution of stresses and pore water pressures during earthquakes. Several studies have shown that low-permeability clay layers overlying sand can inhibit pore water pressure dissipation, thus increasing the risk of liquefaction (Dash & Sitharam, 2009; Sinha et al., 2024). Conversely, dense layers can help reduce pore pressure buildup in underlying loose layers, decreasing the likelihood of liquefaction (Kargar & Osouli, 2024). The presence of thin liquefiable interlayers within predominantly non-liquefiable soil profiles can also alter the overall system response, in terms of both surface deformation and localized vulnerability (Kargar & Osouli, 2024; Sinha et al., 2024).

Other factors that also influence liquefaction potential include soil composition, density, and surface topography. Loose sand with poor gradation (uniform) has a higher liquefaction potential compared to dense soil or well-graded sand (Kim et al., 2024). Irregular topographies such as ridges or valleys can cause stress concentrations that promote pore water pressure buildup and increase liquefaction risk in specific areas (Taslimian et al., 2023)

Liquefaction potential evaluation is carried out by calculating the FS value for each soil layer based on field test data such as SPT and CPT (Purba et al., 2023; Tini et al., 2017) This approach allows for detailed vertical mapping of liquefaction susceptibility, although challenges remain in detecting transitions between soft and stiff layers, particularly in CPT data, which require transition-layer corrections to avoid misinterpretation (Greef & Lengkeek, 2018). Other methods such as shear wave velocity (V_s) measurements and the Dynamic Cone Penetrometer (DCP) are also often used to complement the evaluation (Hashemi & Nikudel, 2016; Patel et al., 2024). Combined approaches integrating multiple test methods with numerical analyses using FEM have become increasingly popular because they can more comprehensively account for inter-layer soil interactions (Halder et al., 2022).

Local studies conducted by Rahayu et al. (2022) showed that soil with certain characteristics in earthquake-prone areas had lower FS values compared to denser soils. This finding is consistent with Nur et al. (2020) who identified a high liquefaction potential in sandy gravel soils with complex stratigraphy in Serpong. These studies demonstrate that accurate liquefaction potential evaluation requires a detailed understanding of subsurface stratigraphy to achieve reliable and safe designs.

Based on this background, this study aims to analyze the liquefaction potential at a location in Semarang Regency, Central Java. The analysis was conducted using SPT data and the CSR-CRR approach according to the

methods of Seed & Idriss (1971) and Youd & Idriss (2001). The evaluation was carried out for three earthquake scenarios with magnitudes of 5.0, 5.9, and 6.5, which represent variations in seismic intensity in the study area.

Similar SPT-based investigations of liquefaction potential have been reported in other regions of Indonesia, such as volcanic sand deposits in Kulonprogo (Artati et al., 2020) and alluvial soils in East Lombok (Ibrohim Burhan et al., 2025). These studies, published in Teknisia Journal, reinforce the relevance of local site characterization and provide methodological context for the present research, which focuses on layered volcanic-colluvial deposits at the southern margin of the Semarang Basin an area rarely examined in previous liquefaction study.

The results of this study are expected to provide fundamental data to support the planning and design of transportation infrastructure, particularly toll roads in earthquake-prone areas, and to provide input for determining effective mitigation measures.

Methodology

Site Description and Data Source

The study was conducted in Bawen District, Semarang Regency, which lies on the southern flank of the Semarang Basin at the northern foot of Mount Ungaran. Geologically, the area is underlain by weathered volcanic and colluvial deposits (Q_{cv}) derived from the Ungaran volcanic complex, overlying Miocene sedimentary rocks of the Kerek Formation. The near-surface layers consist mainly of fine-grained clayey sand, silty sand, and sandy silt with high natural moisture and low density, behaving as reworked volcanic-colluvial materials. These loose and saturated deposits are considered susceptible to ground deformation and liquefaction under strong earthquake shaking.

Subsurface data were obtained from two boreholes (BH-13 and BH-14) drilled within Section 6 of the Toll Road Project, all located

within the administrative area of Bawen, Semarang Regency (e.g., BH-14: X = 0439708; Y = 9198079; UTM Zone 49S). The borehole locations are shown in Figure (1).

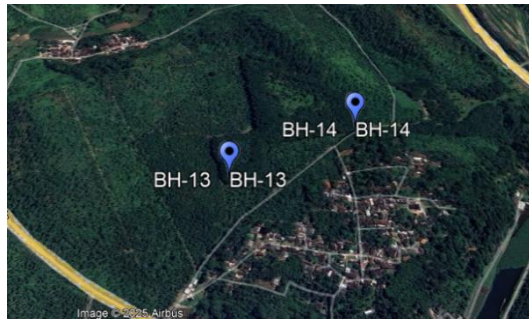


Figure 1. Location map and borehole distribution (BH-13 and BH-14) in Bawen, Semarang Regency.

Each borehole record includes Standard Penetration Test (SPT) N-values, lithological logs, and laboratory test results such as grain-size distribution and Atterberg limits.

The stratigraphy generally consists of alternating silty sand, sandy silt, and clayey silt layers of varying consistency and density. The groundwater table (GWT) was identified from the borehole logs and verified during field observation. Layers below the GWT were assumed to be fully saturated, whereas near surface layers were considered potentially saturated due to capillary or perched-water effects.

Among the two boreholes, BH-14 was selected as the representative profile because it provides a complete set of laboratory data (UDS-1 to UDS-3) and exhibits a clear stratigraphic sequence consistent with BH-13 in the upper 10 m. The raw SPT blow counts (N) from BH-14 were used as the primary input for liquefaction analysis. Corrections for SPT data and stress parameters follow Youd et al. (2001) and are detailed in Section 2.3.2.

Identification of Liquefiable Soil

The preliminary screening of potentially liquefiable soils was carried out using three basic criteria: grain-size distribution, plasticity, and relative density.

First, the grain-size distribution of each soil layer was evaluated with reference to the boundaries proposed by Tsuchida (1970) to identify zones dominated by sandy or silty materials that are generally prone to liquefaction.

Second, the plasticity index (PI) was verified following the criteria of Seed et al. (2003). Fine-grained soils with $PI < 20$ and natural water content (w_n) exceeding the plastic limit (PL) were considered potentially susceptible to liquefaction. Fine-grained layers with moderate PI and $w_n > PL$ were also flagged as potentially susceptible (plastic-fines sands) for detailed FS evaluation.

Finally, the relative density (Dr) was estimated from empirical correlations with the normalized SPT value $(N1)_{60}$. Layers with $Dr < 75\%$ were classified as loose to medium-dense and thus considered potentially liquefiable.

In layered profiles where silty-clay interbeds alternate with sandy/silty-sand horizons, only the granular sublayers that satisfy the Seed et al. (2003) screening (low to moderate PI and $w_n > PL$) were treated as potentially susceptible. Clayey interbeds with moderate PI were interpreted as non-liquefiable (clay-like behavior), although they may contribute to cyclic softening and pore-pressure trapping.

These screening criteria were used only to preliminarily identify potentially susceptible layers, whereas the final assessment of liquefaction potential was determined from the SPT-based Factor of Safety (FS) analysis using the CSR–CRR approach. The Atterberg-limit and grain-size criteria thus served as supporting indicators to delineate the critical intervals for detailed evaluation.

Liquefaction Analysis

Based on the identified susceptible layers, the liquefaction potential was further evaluated using the simplified procedure proposed by Seed and Idriss (1971) and its subsequent updates by Seed et al. (1985) and Youd et al. (2001). This approach compares the cyclic

stress ratio (CSR) induced by the design earthquake with the cyclic resistance ratio (CRR) of the soil, which represents its capacity to resist liquefaction. The method was selected due to its proven reliability and widespread application in SPT-based liquefaction assessments for sandy and silty soils.

Because SPT N-values represent an averaged response over the sampling interval, thin interlayers may not be fully resolved. Therefore, FS values reported for a mixed layer represent a conservative assignment to the governing granular sublayer within that interval, while cohesive sublayers are not assumed to liquefy.

Simplified Evaluation of CSR and CRR

The cyclic stress ratio (CSR) represents the seismic shear stress induced in the soil during an earthquake and was computed using the simplified formulation proposed by Seed and Idriss (1971) on Eq. (1),

$$CSR = \frac{T_{av}}{\sigma'_{vo}} = 0.65 \left(\frac{a_{max}}{g} \right) \left(\frac{\sigma_{vo}}{\sigma'_{vo}} \right) r_d \quad (1)$$

where a_{max} is the peak horizontal ground acceleration, g is gravitational acceleration, σ_{vo} and σ'_{vo} are total and effective overburden stresses. The stress reduction factor (r_d) was calculated using the empirical equation proposed by T.F. Blake (1996) as cited in Youd & Idriss (2001). This formulation accounts for the flexibility of the soil column and is applicable for routine liquefaction evaluation up to 30 m depth.

Peak ground acceleration (PGA) at the ground surface, a_{max} , was determined following the SNI 03-1726:2002 seismic zoning approach to ensure consistency with the accompanying undergraduate thesis dataset. The site is located in Zone 3 where the bedrock acceleration (S_{PGA}) is 0.30 g. Considering a local site amplification factor $F_{PGA} = 1.20$ for soft to medium soil conditions, the surface acceleration is calculated $a_{max} = F_{PGA} \times S_{PGA} = 1.20 \times 0.30g = 0.36g$. This a_{max} value was then used in the CSR computation together with the total and effective

overburden stresses ($\sigma_{vo}, \sigma'_{vo}$) as described by Blake (1996), as cited in Youd & Idriss (2001).

The cyclic resistance ratio (CRR) was determined from the corrected SPT blow count $(N1)_{60}$ using the correlation proposed by Seed et al. (1985) and updated by Youd et al. (2001) for a magnitude $M_w = 7.5$ reference earthquake. The CRR was then adjusted for actual earthquake magnitude and overburden stress using the magnitude scaling factor (MSF) and the overburden correction factor (K_σ) using Eq. (2).

$$CRR_M = CRR_{7.5} \times MSF \times K_\sigma \quad (2)$$

where MSF accounts for the reduced number of loading cycles in smaller earthquakes (Idriss, 1999), and K_σ reduces the resistance under higher confining pressures.

Correction of SPT Data and Stress Parameters

The field SPT blow counts (N) were corrected to a standardized reference condition to obtain the normalized value $(N1)_{60}$, following Youd et al. (2001). The correction accounted for the effects of equipment, procedures, and in-situ stress conditions using Eq. (3):

$$(N1)_{60} = N_m C_N C_E C_B C_R C_S \quad (3)$$

where N_m is the measured blow count, and C_N, C_E, C_B, C_R, C_S are correction factors.

Value of $C_E = 0.78$, $C_B = 1.00$, $C_R = 1$, and $C_S = 1.00$ were adopted, with C_N computed as a function of overburden stress (Youd et al., 2001). The resulting $(N1)_{60}$ values range from approximately 4 to 13 within the upper 15 m, representing loose to medium-dense layers that were evaluated for liquefaction potential. Below 15 m, $(N1)_{60} > 20$, indicating stiff, non-liquefiable soils.

Evaluation of Factor of Safety and Interpretation Criteria

The factor of safety (FS) against liquefaction was evaluated as the ratio between the cyclic resistance ratio (CRR) and the cyclic stress ratio (CSR) using Eq. (4):

$$FS = \frac{CRR_{Mw}}{CSR} \quad (4)$$

Layers with $FS < 1.0$ are considered potentially liquefiable, those with $1.0 \leq FS \leq 1.2$ marginally stable, and those with $FS > 1.2$ stable (Seed et al., 1985; Youd & Idriss, 2001).

For interpretative clarity, the computed FS values were plotted against depth to identify the zones of liquefaction potential.

Earthquake Scenarios

Three earthquake magnitudes ($M_w = 5.0, 5.9, 6.5$) were analyzed based on historical events in Central Java and the seismic hazard zoning of SNI 03-1726:2002. These scenarios were used to evaluate the sensitivity of the site to different earthquake intensities, with CSR and CRR compared for each magnitude to delineate the depth and extent of potentially liquefiable zones

Flowchart of Analysis Procedure

The systematic analysis from SPT correction and CSR-CRR calculation to FS evaluation is illustrated in the flowchart (Figure (2)).

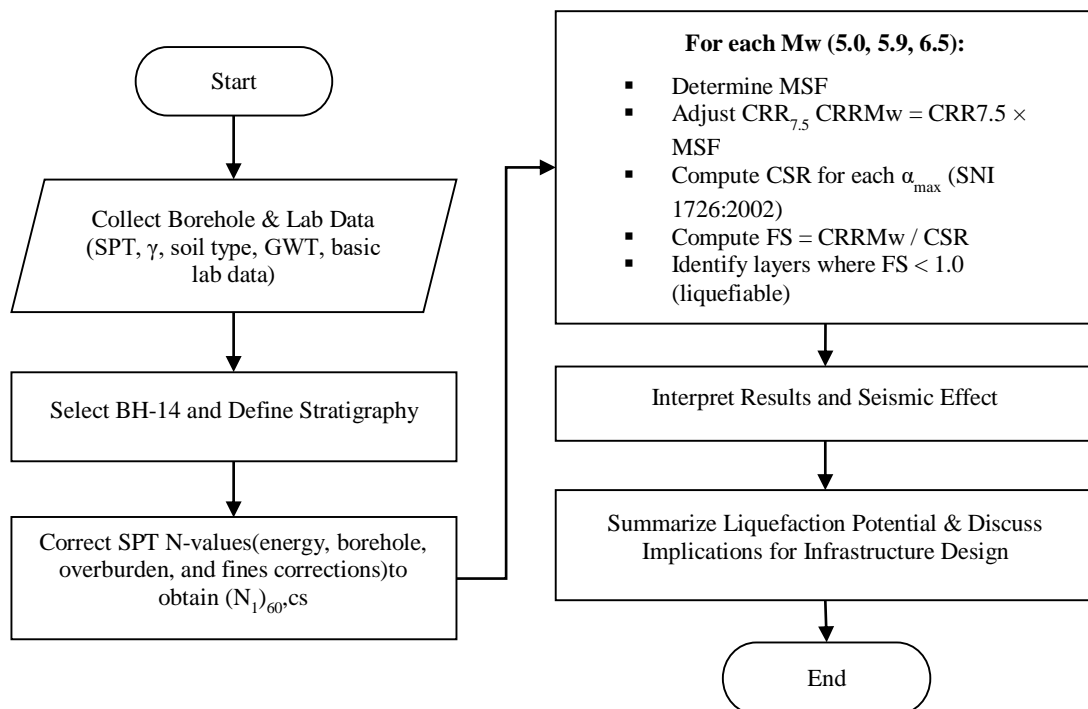


Figure 2. Flowchart of the SPT-based liquefaction evaluation procedure

Results

The discussion stages of the research results are soil stratigraphy, grain size and plasticity characteristics and liquefaction potential analysis.

Soil Stratigraphy

Borehole BH-14 ($X = 0439708, Y = 9198079$) is located near the Ungaran-Bawen Toll Road within the volcanic-colluvial deposits (Qcv) that overlie the Miocene Kerek Formation. These deposits consist mainly of fine sand, silt, and clay derived from reworked volcanic materials originating from the Ungaran volcanic complex. The borehole log shows loose clayey sand and silty sand in the upper 0-8 m, underlain by stiff silty clay extending to approximately 27 m depth. SPT N-values range from 3-7 in the upper sandy layers and increase beyond 20 in the deeper cohesive layers, indicating a transition from loose to dense soil (Figure (3)).

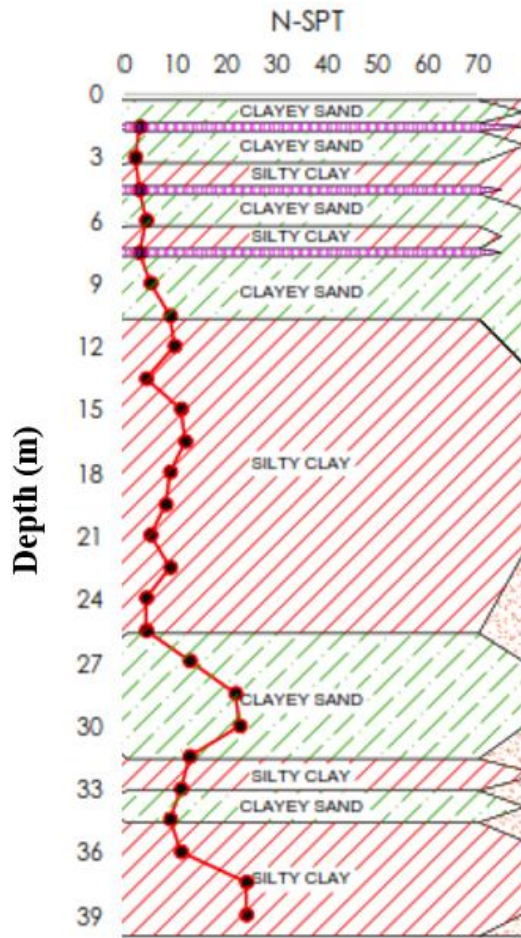


Figure 3. Soil stratigraphy and SPT N-Value profile of BH-14

The groundwater table (GWT) recorded at 27 m likely represents the delayed stabilization level after drilling rather than the actual phreatic surface. This interpretation is supported by (i) high degrees of saturation ($S_r = 87-98\%$) and natural moisture contents in the upper silty-sand layers, and (ii) adjacent BH-13 showing a shallower GWT of 14 m. Such discrepancies are common in volcanic-colluvial terrains, where alternating permeable and less-permeable layers can produce perched groundwater and shallow saturation zones (Fadillah et al., 2023). Therefore, the actual phreatic level is interpreted to be shallow (2-3 m), consistent with local conditions.

Grain Size and Plasticity Characteristics

Laboratory tests on UDS-1 (1-1.5 m), UDS-2 (4-4.5 m), and UDS-3 (7-7.5 m) indicate fines contents of 53-60 %, plasticity indices (PI) of 13-16, and degrees of saturation (S_r) of 87-98 % (Table (1)). With $w_n > PL$ and moderate PI, these silty-sand/clayey-sand layers are not classic clay-like liquefiable soils, but under saturated conditions they are susceptible to cyclic softening, consistent with Seed et al. (2003) screening for plastic-fines sands and with their position between Tsuchida's liquefiable boundaries (Figure (4)). ($LL = 45\%$, not tabulated)

Table 1. Fines Content in BH-14

Depth (m)	Soil Type	Fines (%)	S_r (%)	PI
1.00-1.50	Clayey sand	60.2	87.4	13.5
4.00-4.50	Clayey sand	56.5	98.3	14.4
7.00-7.50	Clayey sand	53.2	92.4	15.8

All samples plot within Tsuchida's (1970) liquefiable range, indicating moderate to high susceptibility (Figure (4)).

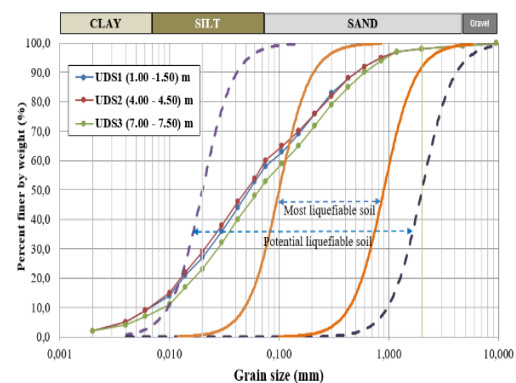


Figure 4. Grain-size distribution of UDS1-UDS3 (BH-14).

Liquefaction Potential Analysis

Liquefaction analysis was conducted using the Simplified Procedure of Seed and Idriss (1971) for three earthquake scenarios ($M_w = 5.0, 5.9, 6.5$) with a surface acceleration $a_{max} = 0.36g$ (from SNI 03-1726:2002, Zone 3). Figures (5) - Figures (7) illustrate the

CSR–CRR relationships and FS profiles for each scenario.

For $M_w = 5.0$, the analysis indicates that the upper 0-3 m sandy layers have FS values between 0.14 and 0.41, confirming their susceptibility to initial liquefaction under moderate shaking, while deeper strata remain stable ($FS > 1.0$).

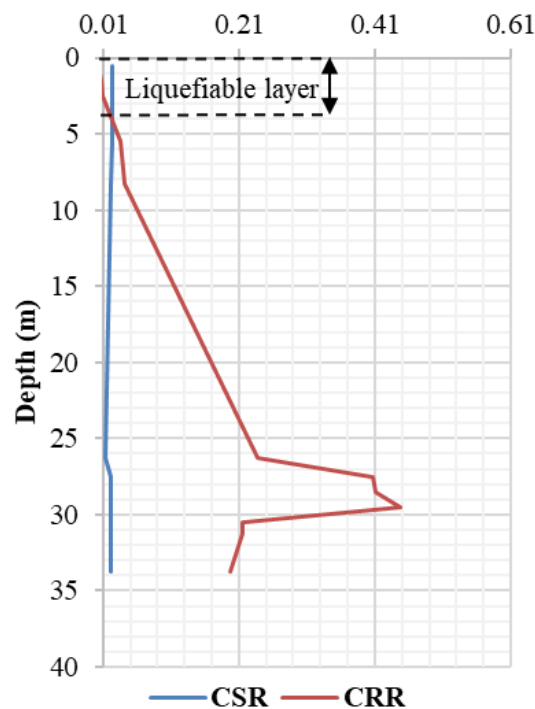


Figure 5. CSR-CRR profile at BH-14 for $M_w = 5.0$

For $M_w = 5.9$, shallow liquefaction remains confined to 0-3 m ($FS = 0.09 - 0.27$), whereas the underlying 4.5-9 m zone shows $FS = 1.0 - 1.2$, indicating marginal stability.

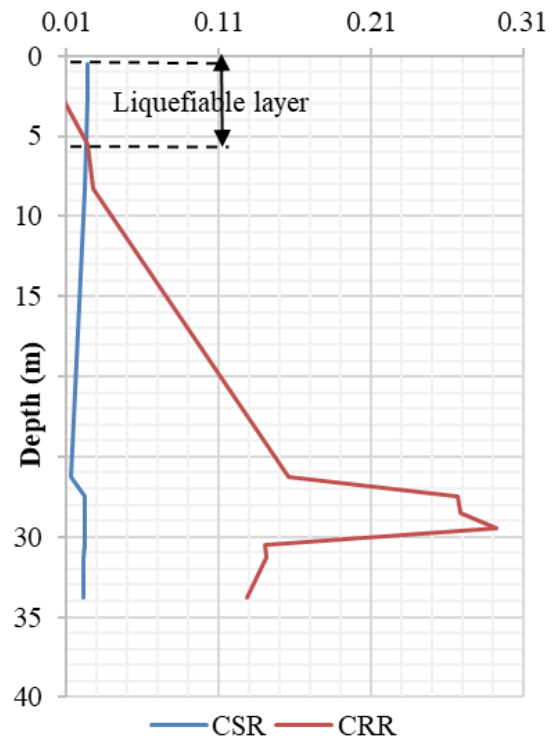


Figure 6. CSR-CRR profile at BH-14 for $M_w = 5.9$

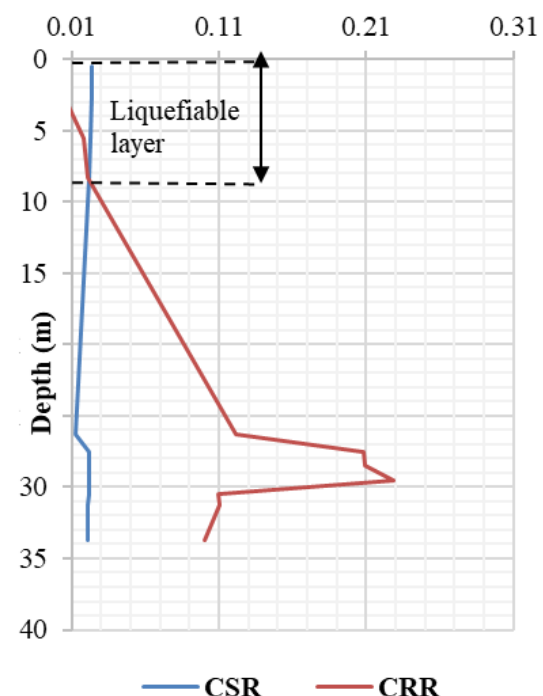


Figure 7. CSR-CRR profile at BH-14 for $M_w = 6.5$

Under $M_w = 6.5$, the liquefiable interval extends to about 9 m, with FS values of 0.07-0.96, denoting high to marginal susceptibility near the surface. Layers deeper than 10 m remain stable ($FS > 1.2$) due to higher density and confining stress. Where $FS < 1$ is observed across a mixed sandy-clayey interval, it represents the controlling sandy sublayer; the interbedded silty clay lenses ($PI = 13-16$) are interpreted as non-liquefiable but may retard drainage and amplify pore-pressure buildup near the surface.

Figure (8) - Figure (10) show the variation of the factor of safety (FS) with depth for the three earthquake scenarios. The plots illustrate that FS values decrease systematically with increasing magnitude, indicating higher seismic demand and pore-pressure buildup in the shallow layers. Table (2) summarizes the representative FS ranges and corresponding liquefaction potential for each depth interval

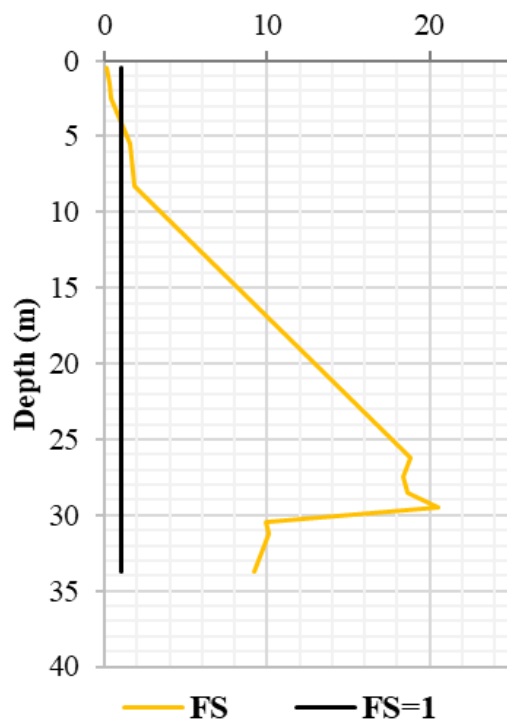


Figure 8. Factor of safety (FS) profiles at BH-14 for $M_w = 5.0$. FS represents the controlling granular sublayer within each mixed interval.

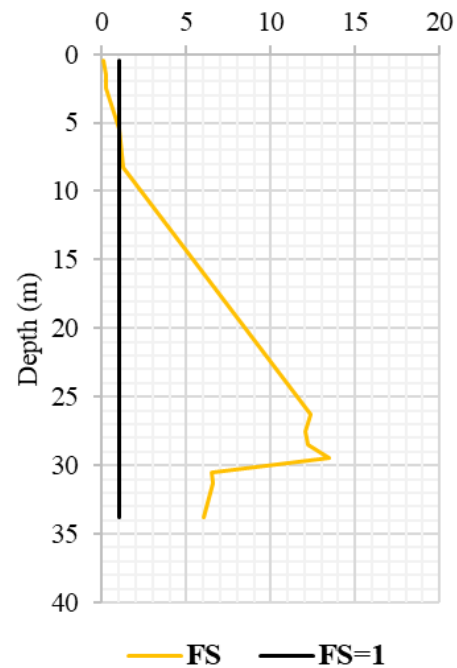


Figure 9. Factor of safety (FS) profiles at BH-14 for $M_w = 5.9$. FS represents the controlling granular sublayer within each mixed interval.

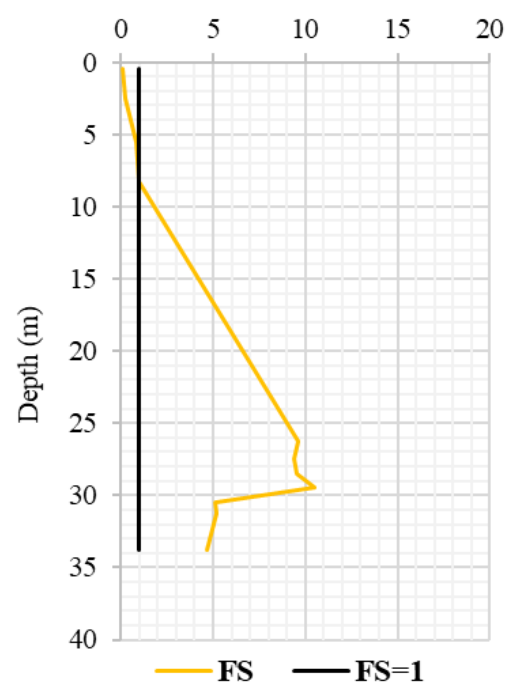


Figure 10. Factor of safety (FS) profiles at BH-14 for $M_w = 6.5$. FS represents the controlling granular sublayer within each mixed interval.

The apparent deep liquefiable zone (27 m) identified in earlier plots was found to be an interpolation artifact, since that layer

corresponds to stiff silty clay ($N > 20$) with moderate plasticity, indicating non-liquefiable behavior. Therefore, the shallow silty-sand layers represent the dominant liquefiable horizons under strong seismic loading

Table 2. Summary of factor of safety (FS) values at BH14 for different earthquake scenarios

Earthquake Magnitude	Depth (m)	FS Range	Liquefaction Potential
Mw = 5.0	0 - 3	0.14 - 0.41	Liquefiable
	> 3	> 1.0	Safe
Mw = 5.9	0 - 3	0.09 - 0.27	Liquefiable
	4.5 - 6	1.23	Stable
	6 - 9	1.02	Marginal
	> 10	> 1.2	Safe
Mw = 6.5	0 - 3	0.07 - 0.21	Liquefiable
	4.5 - 9	0.80 - 0.96	Marginally Liquefiable
	> 10	> 1.2	Safe

These findings are consistent with Jefferies and Been (2016), who emphasized that liquefaction susceptibility is governed by density and effective confining stress.

Influence of Groundwater Depth and Seismic Demand

The previous analysis showed that the lowest liquefaction safety factors occur in the upper layers, with $FS = 0.14-0.41$ ($M_w = 5.0$) and $FS = 0.09-0.27$ ($M_w = 5.9$) at 0-3 m, and $FS = 0.07-0.21$ ($M_w = 6.5$) at the same depth; the 4.5-9 m interval becomes marginal ($FS = 0.80-0.96$) for $M_w = 6.5$, while >10 m remains stable ($FS > 1.2$).

Although the groundwater level was measured at approximately 27 m, field and laboratory evidence suggests that the alternating silty-sand and clayey layers promote perched groundwater and shallow phreatic conditions within the upper deposits. This interpretation is supported by high natural moisture contents and degrees of saturation ($S_r = 87-98\%$) in near surface samples and is consistent with hydrogeological characteristics of volcanic-colluvial terrains reported by Fadillah et al. (2023)

Consequently, the near-surface sandy layers remain the most critical zone, where cyclic stress ratios (CSR) exceed the cyclic resistance ratio (CRR), resulting in FS values below unity under strong shaking ($M_w \geq 5.9$).

These findings confirm that the apparent deep groundwater measurement does not represent the true hydrogeological condition and that shallow liquefaction can still occur during strong seismic events, consistent with the adjacent BH-13 indicating a much shallower groundwater table (14 m).

Discussions

The analysis confirms that the upper 0-9 m sandy layers constitute the principal liquefiable horizons under strong earthquake loading ($M_w \geq 5.9$), with computed safety factors ranging from 0.7 to 0.95. In contrast, the deeper deposits (> 10 m) are denser and yield $FS > 1.2$, indicating stable, non-liquefiable behavior.

The interpreted shallow perched groundwater level (2-3 m), supported by high natural moisture and near-saturation in the upper samples, explains the observed cyclic softening potential.

Overall, the site can be classified as moderately susceptible to shallow liquefaction, where loose sandy layers and localized perched groundwater govern the soil response under seismic loading.

Implications for Infrastructure Planning

The identification of liquefiable layers at shallow depths has direct implications for the design and maintenance of the toll road corridor. Liquefaction-induced ground deformation, such as settlement and lateral spreading, could compromise embankment stability and pavement performance. For sites with BH-14 type soils, differential settlement may cause surface cracking and reduced serviceability if untreated.

To mitigate these risks, ground improvement should be integrated at the design stage, particularly within the upper 0-9 m sandy layers identified as critical. Recommended methods include:

- Soil densification for shallow sandy deposits (< 5 m);
- Stone columns or Prefabricated Vertical Drains (PVD) with preloading to accelerate consolidation and increase density; and
- Deep Soil Mixing (DSM) for critical sections requiring higher stiffness and shear strength.

These methods have been shown to increase the factor of safety by 30-50% in comparable projects (Can et al., 2024; Huang et al., 2016a), and their application in the Semarang-Bawen corridor would reduce liquefaction susceptibility and improve the seismic resilience of this toll road section.

Conclusion

The SPT-based liquefaction analysis shows that the shallow sandy layers at BH-14 (0-9 m) are the most vulnerable to cyclic loading. For $M_w = 5.0$, the 0-3 m layer already yields $FS = 0.14-0.41$ (<1), indicating liquefaction susceptibility. For $M_w = 5.9$, 0-3 m remains $FS = 0.09-0.27$, while 4.5-9 m is marginal to stable ($FS = 1.0-1.2$). For $M_w = 6.5$, 0-3 m drops to $FS = 0.07-0.21$ and 6-9 m becomes marginal ($FS = 0.80-0.96$), whereas >10 m remains stable ($FS > 1.2$) due to higher density and effective confining stress.

Although the bore log recorded a groundwater level at 27 m, field and laboratory indicators ($S_r = 87-98\%$) and data from the adjacent BH-13 (GWT = 14 m) suggest a shallow phreatic or perched groundwater condition within the upper deposits. This interpretation reconciles the deep GWT measurement with the observed shallow susceptibility.

Intervals showing $FS < 1$ within mixed sandy-clayey layers correspond to the controlling granular sublayers, while clayey lenses with moderate plasticity are non-liquefiable but

may impede drainage and amplify pore-pressure build-up.

Applying updated seismic demand from SNI 1726:2019 would further increase CSR and reduce FS in these shallow layers, though the critical depth range remains within 0-9 m.

Overall, the site is moderately susceptible to shallow liquefaction, where loose sandy layers and shallow groundwater conditions govern the seismic response

Acknowledgments

The authors would like to express their sincere gratitude to Bambang Suharyadi, S.T., M.T., Director of PT Tunas Lima Warna, for kindly providing the geotechnical investigation data used in this study. His support was invaluable in enabling the completion of this research.

References

- Agustina, S. (2024). Liquefaction Potential Analysis in Terboyo Industrial Park. *IOP Conference Series: Earth and Environmental Science*, 1321(1). <https://doi.org/10.1088/1755-1315/1321/1/012006>
- Artati, H. K., Pawirodikromo, W., & Purwanto, E. (2020). Analisis Potensi Likuifaksi pada Pasir Vulkanik di Pantai Glagah Kulonprogo Berdasarkan Data N-SPT. *Teknisia*, XXV(2), 50–62. <https://doi.org/10.20885/teknesia.vol25.iss2.art6>
- Can, A., Celenk, B., Mursal, U., Tunar Özcan, N., & Gokceoglu, C. (2024). Performance Assessment of Deep Soil Mixing Columns Against Liquefaction Problem in a Railway Embankment. *Indian Geotechnical Journal*, 54(6), 2240–2258. <https://doi.org/10.1007/s40098-023-00860-y>
- D'Apuzzo, M., Evangelisti, A., Modoni, G., Spacagna, R. L., Paoletta, L., Santilli, D., & Nicolosi, V. (2020). Simplified Approach for Liquefaction Risk Assessment of Transportation Systems: Preliminary Outcomes. *Lecture Notes in Computer Science (Including Subseries Lecture Notes in Artificial Intelligence and Lecture Notes in Bioinformatics)*, 12255 LNCS(September), 130–145. https://doi.org/10.1007/978-3-030-58820-5_10
- Dash, H. K., & Sitharam, T. G. (2009). Undrained cyclic pore pressure response of sand-silt mixtures: Effect of nonplastic fines and other parameters. *Geotechnical and Geological Engineering*, 27(4),

- 501–517. <https://doi.org/10.1007/S10706-009-9252-5>
- Fadillah, A., Harijoko, A., Hendrayana, H., Wibowo, H. E., Baud, B., Lachassagne, P., Muhammad, A. S., & Dörfliger, N. (2023). Hydrogeological Interpretation Using Electrical Resistivity Tomography: Methodology and Conceptual Model in Andesitic Volcanic Context. *International Journal of GEOMATE*, 24(106), 25–36. <https://doi.org/10.21660/2023.106.3728>
- Fajarwati, Y., Sasmayaputra, N. A., Wibowo, D. E., & Endaryanta. (2025). Evaluating Liquefaction Potential and Ground Reinforcement Strategies for Railway Infrastructure in Coastal South Sulawesi. *IOP Conference Series: Earth and Environmental Science*, 1488(1). <https://doi.org/10.1088/1755-1315/1488/1/012077>
- Gallant, A. P., Montgomery, J., Mason, H. B., Hutabarat, D., Reed, A. N., Wartman, J., Irsyam, M., Simatupang, P. T., Alatas, I. M., Prakoso, W. A., Djarwadi, D., Hanifa, R., Rahardjo, P., Faizal, L., Harnanto, D. S., Kawanda, A., Himawan, A., & Yasin, W. (2020). The Sibalaya flowslide initiated by the 28 September 2018 MW 7.5 Palu-Donggala, Indonesia earthquake. *Landslides*, 17(8), 1925–1934. <https://doi.org/10.1007/s10346-020-01354-1>
- Greef, J. de, & Lengkeek, H. J. (2018). Transition and thin layer corrections for CPT based liquefaction analysis. *Proceedings Of The 4th International Symposium On Cone Penetration Testing (CPT'18)*, 317–322.
- Halder, A., Das, K., Nandi, S., & Bandyopadhyay, K. (2022). A comparative study on liquefaction assessment of Rajarhat area of Kolkata by using different approaches. *Cone Penetration Testing 2022 - Proceedings of the 5th International Symposium on Cone Penetration Testing, CPT 2022*, 955–960. <https://doi.org/10.1201/9781003308829-143>
- Hashemi, M., & Nikudel, M. R. (2016). Application of Dynamic Cone Penetrometer test for assessment of liquefaction potential. *Engineering Geology*, 208, 51–62. <https://doi.org/10.1016/j.enggeo.2016.04.013>
- Huang, C., Sui, Z., Wang, L., & Liu, K. (2016a). Mitigation of Soil Liquefaction Using Stone Columns: An Experimental Investigation. *Marine Georesources & Geotechnology*, 34(3), 244–251. <https://doi.org/10.1080/1064119X.2014.1002872>
- Huang, C., Sui, Z., Wang, L., & Liu, K. (2016b). Mitigation of Soil Liquefaction Using Stone Columns: An Experimental Investigation. *Marine Georesources and Geotechnology*, 34(3), 244–251. <https://doi.org/10.1080/1064119X.2014.1002872>
- Ibrohim Burhan, L., Kusuma Artati, H., Makrup, L., & Saputra, E. (2025). Liquefaction potential study under Ijo Balit weir in East Lombok Indonesia. *Teknisia*, 30(1), 23–32. <https://doi.org/10.20885/teknisia.vol30.iss1.art3>
- Jefferies, M., & Been, K. (2016). *Soil Liquefaction: A Critical State Approach* (William Powrie (ed.); Second Edi). CRC Press.
- Kargar, P., & Osouli, A. (2024). Liquefiable Interlayer Effects in a Liquefaction-Susceptible Site. *Geo-Congress 2024*, 250–258. <https://doi.org/10.1061/9780784485316.027>
- Kim, J., Athanasopoulos-Zekkos, A., & Zekkos, D. (2024). The Effect of Initial Static Shear Stress on Liquefaction Triggering of Coarse-Grained Materials. *Journal of Geotechnical and Geoenvironmental Engineering*, 150(10). <https://doi.org/10.1061/JGGEFK.GTENG-12282>
- Kusumah, A. W. (2018). *Di Balik Pesona Palu - Bencana Melanda Geologi Menata* (Andiani, O. Oktariadi, & A. Kurnia (eds.); Vol. 1). Badan Geologi.
- Kusumayudha, S. B., Markam, A. P., & Rahmat, B. (2011). Structure, hydrogeology, and the geothermal system of Mount Ungaran area, Central Java, Indonesia. *Proceeding of 15th International Conference of Women Engineers and Scientists, Figure 1*, 1–10.
- Moderie, J., & Rippe, A. H. (2009). Seismic Hazards and Construction Vibrations. *Contemporary Topics in Deep Foundations*, 327–334. [https://doi.org/10.1061/41021\(335\)41](https://doi.org/10.1061/41021(335)41)
- Nur, S. H., Hafid, A., & Iswanto, E. R. (2020). Liquefaction potentials analysis of sandy gravel on the sediment deposit of the Serpong formation. *IOP Conference Series: Earth and Environmental Science*, 419(1). <https://doi.org/10.1088/1755-1315/419/1/012081>
- Nurdin, S. (2019). *Nalodo dan Konsep Rehabilitasi dan Rekonstruksi Saluran Irigasi Gumbasa*.
- Pal, S., & Deb, K. (2018). Effect of Stiffness of Stone Column on Drainage Capacity during Soil Liquefaction. *International Journal of Geomechanics*, 18(3), 1–11. [https://doi.org/10.1061/\(asce\)gm.1943-5622.0001108](https://doi.org/10.1061/(asce)gm.1943-5622.0001108)
- Patel, N., Ahamad, M. N., & Singh, V. P. (2024). *A Comprehensive Study on Seismic Site Characterization and Liquefaction Susceptibility Assessment (LSA) through Multi-channel Analysis of Surface Wave (MASW)*. 0–12.

- <https://www.researchsquare.com/article/rs-4388341/v1>
- Purba, S. F., Ismanti, S., & Setiawan, A. F. (2023). Liquefaction potential analysis in Yogyakarta Bawen Toll Road section 3. *E3S Web of Conferences*, 429, 1–11. <https://doi.org/10.1051/e3sconf/202342904020>
- Rahayu, A., Uno, I., Hidayat, N., Dwijaka, A., & Yusuf, M. (2022). Potential of Liquefaction at Nasanapura Hospital Petobo Village Palu City. *IOP Conference Series: Earth and Environmental Science*, 1075(1). <https://doi.org/10.1088/1755-1315/1075/1/012028>
- Salem, Z. Ben, Frikha, W., & Bouassida, M. (2017). Effects of Densification and Stiffening on Liquefaction Risk of Reinforced Soil by Stone Columns. *Journal of Geotechnical and Geoenvironmental Engineering*, 143(10), 1–6. [https://doi.org/10.1061/\(asce\)gt.1943-5606.0001773](https://doi.org/10.1061/(asce)gt.1943-5606.0001773)
- Seed, H. B., & Idriss, I. M. (1971). Simplified procedure for evaluating soil liquefaction potential. *J. Soil Mech. Found. Div. Am. Soc. Civ. Eng.*, 97(9), 1249–1273.
- Seed, H. B., Tokimatsu, K., Harder, L. F., & Chung, R. M. (1985). The influence of SPT procedures in soil liquefaction resistance evaluations. *Journal of Geotechnical Engineering*, 111(12), 15.
- Sinha, S. K., Ziotopoulou, K., & Kutter, B. L. (2024). Effects of Excess Pore Pressure Redistribution in Liquefiable Layers. *Journal of Geotechnical and Geoenvironmental Engineering*, 150(4). <https://doi.org/10.1061/JGGEFK.GTENG-11857>
- Taslimian, R., Noorzad, A., & Maleki Javan, M. R. (2023). Numerical Analysis of Liquefaction Phenomenon Considering Irregular Topographic Interfaces Between Porous Layers. *Journal of Earthquake Engineering*, 27(5), 1095–1109. <https://doi.org/10.1080/13632469.2022.2038727>
- Tini, T., Tohari, A., & Iryanti, M. (2017). Analisis Potensi Likuifaksi Akibat Gempa Bumi Menggunakan Metode SPT (Standar Penetration Test) Dan Cpt (Cone Penetration Test) Di Kabupaten Bantul, Yogyakarta. *Wahana Fisika*, 2(1), 8. <https://doi.org/10.17509/wafi.v2i1.7022>
- Wicaksono, A., Hardiyatmo, H. C., & Satyarno, I. (2024). Evaluation of the Impact of Liquefaction Potential on the Construction of the Solo - Yogyakarta - NYIA Kulon Toll Road. *IOP Conference Series: Earth and Environmental Science*, 1373(1). <https://doi.org/10.1088/1755-1315/1373/1/012006>
- Widiarso, D. A., Herlambang, F. G. S., Trisnawati, D., Qadaryati, N., & Haryanto, W. (2025). Soil Bearing Capacity Analysis To Determine Pile Foundation Design on Alluvial Soils in Semarang City, Indonesia. *International Journal of GEOMATE*, 28(129), 10–20. <https://doi.org/10.21660/2025.129.3732>
- Widiyanto, W., Santoso, P. B., Hsiao, S.-C., & Imananta, R. T. (2019). Post-event Field Survey of 28 September 2018 Sulawesi Earthquake and Tsunami. In *Natural Hazards and Earth System Sciences Discussions* (pp. 1–23). <https://doi.org/10.5194/nhess-2019-91>
- Youd, T. L., & Idriss, I. M. (2001). Liquefaction resistance of soils: Summary report from the 1996 NCEER and 1998 NCEER/NSF workshops on evaluation of liquefaction resistance of soils. *Journal of Geotechnical and Geoenvironmental Engineering*, 127(4), 297–313. [https://doi.org/10.1061/\(ASCE\)1090-0241\(2001\)127:4\(297\)](https://doi.org/10.1061/(ASCE)1090-0241(2001)127:4(297))